

Parametrized Physics-Informed Neural Operators for Lithium-Ion-Battery Modeling

Philipp Brendel¹, Andreas Rosskopf¹, and Vincent Lorentz^{1,2}

philipp.brendel@iisb.fraunhofer.de

¹ Fraunhofer Institute for Integrated Systems and Device Technology IISB, Erlangen, Germany

² Chair of Electronics for Electrical Energy Storage, University of Bayreuth, Germany



Introduction

- Accurate and reliable state estimation for Lithium-Ion-Battery (LIB) cells can be achieved through successful parametrization of suitable LIB surrogate models [1].
- Nondestructive parametrization, e.g., based on measured current and voltage data, requires sophisticated approaches with high computational efforts for parameter evaluations, sensitivity analyses and optimized Design-of-Experiments (DoE) [2].
- Parametrized Neural Operators offer the potential to reduce these efforts by providing surrogate models that can be used more efficiently, e.g. in on-board state estimation for electric vehicles, after a significant training effort.

Methodology

Single-Particle-Model:

- Partial Differential Equation (PDE) to describe Li-concentration $c_j(r, t)$ in two spherically symmetric particles for anode (j=n) and cathode (j=p):

$$\frac{\partial c_j(r, t)}{\partial t} = \frac{D_j}{r^2} \frac{\partial}{\partial r} \left(r^2 \frac{\partial c_j(r, t)}{\partial r} \right).$$

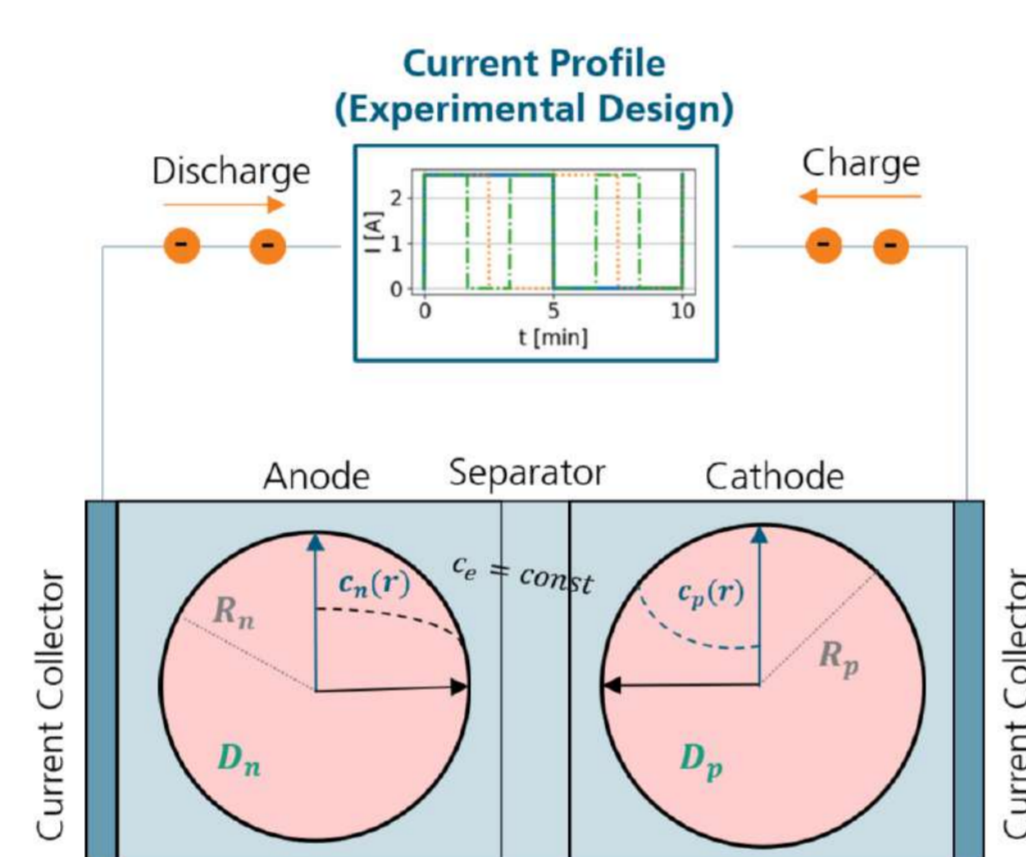


Figure 1: Single-Particle-Model.

- Initial (IC) and Boundary Conditions (BCs):

$$c_j(r, 0) = c_j^0, \quad \frac{\partial c_j(0, t)}{\partial r} = 0, \quad \frac{\partial c_j(R_j, t)}{\partial r} = \pm \frac{I(t)}{A_L j F D_j a_j}.$$

- Model parameters as characterized for a cylindrical LGM50 cell [3].

Physics-Informed Deep Operator Network (PI-DeepONet):

- Data-free training via minimization of PDE, IC and BC residuals
- Branch network: Encoding discretized current profiles ($I_{t_0}, I_{t_1}, \dots, I_{t_{600}}$) that are generated from Gaussian Random Fields (GRF), cf. Fig. 2.
- Trunk network: Encoding spatio-temporal and diffusivity domain (r, t, D_n, D_p)

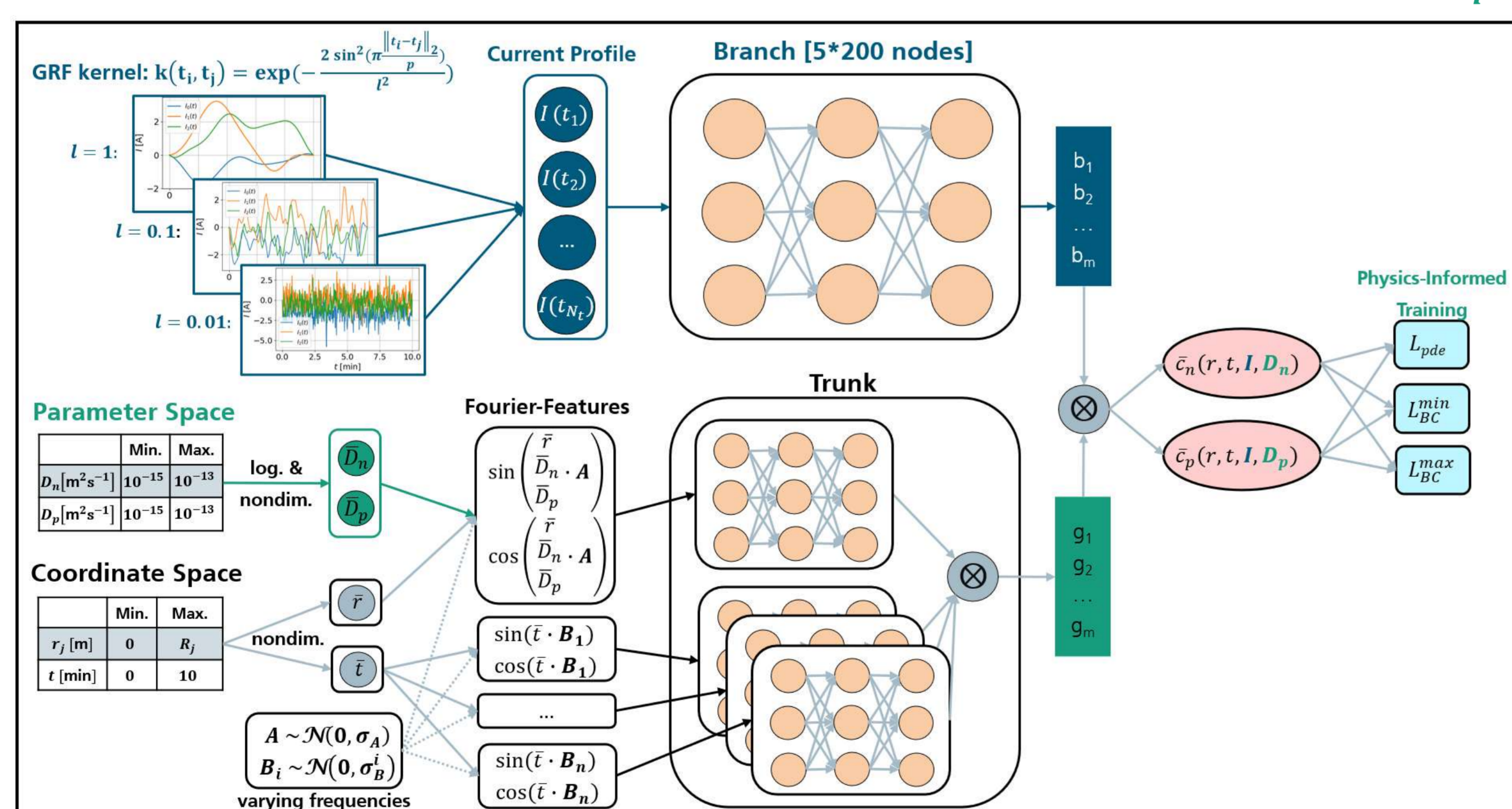


Figure 2: Single-Particle-Model.

Error metric:

- Normalized-Mean-Absolute-Percentage-Error at particle surfaces computed with respect to a numerical reference solution obtained via Finite-Differences:

$$\text{NMAPE}^{\text{surf}} = \frac{1}{2} \sum_{j \in \{n, p\}} \frac{1}{N_t} \sum_{i=0}^{N_t} \frac{|c_j^{\text{NN}}(R_j, t_i) - c_j^{\text{ref}}(R_j, t_i)|}{\max\{c_j^{\text{ref}}(R_j, t)\} - \min\{c_j^{\text{ref}}(R_j, t)\}} \cdot 100\%.$$

Results

Surrogate Model Accuracy:

- Best result after training ~4 days on a NVIDIA A100: **0.8% NMAPE^{surf}_{avg}** (avg. on 9 GRF profiles and 121 samples $(D_n, D_p) \in [10^{-15}, 10^{-13}]^2$)

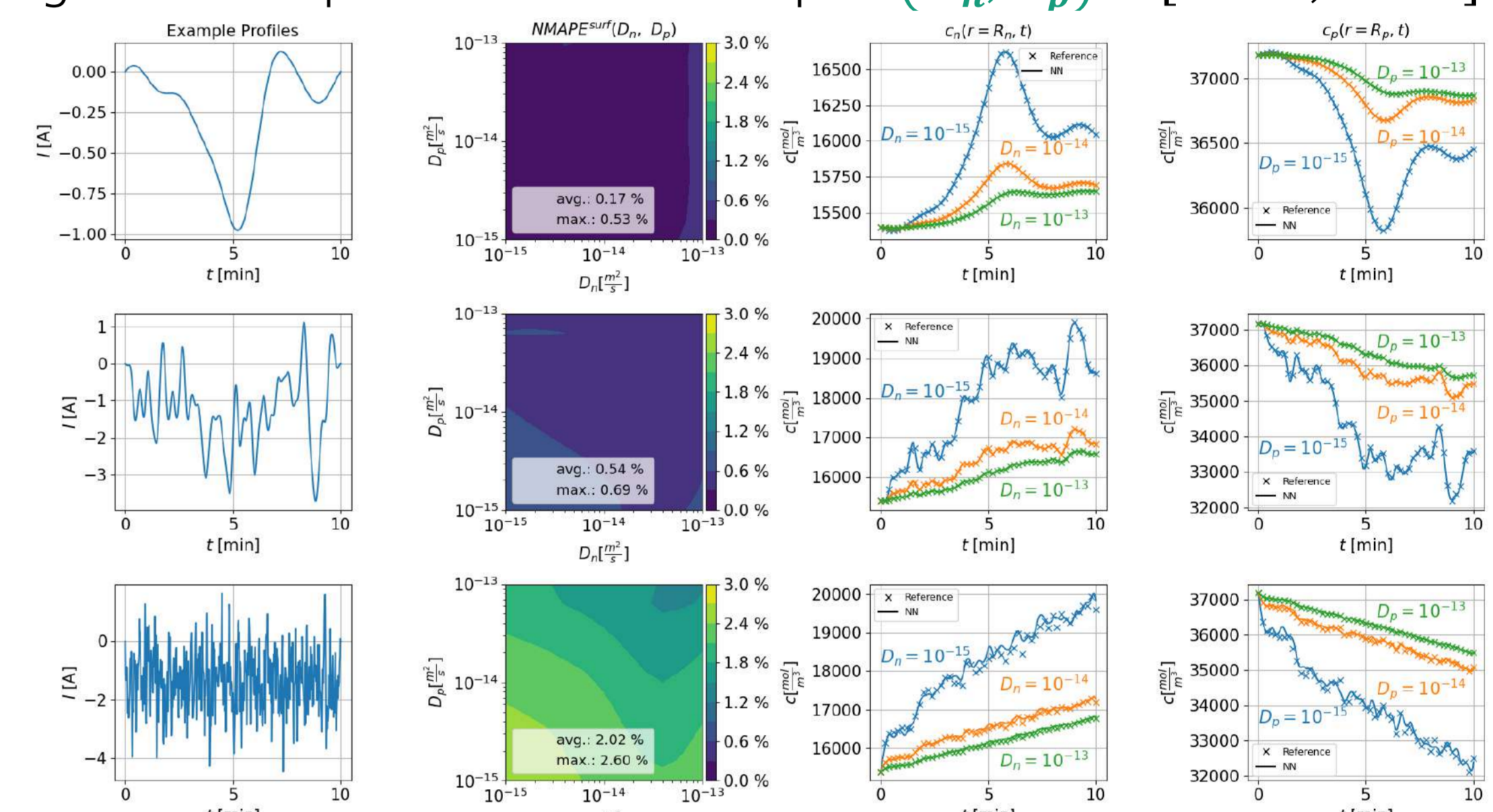


Figure 3: Surrogate model accuracy on three exemplary GRF profiles across diffusivity domain.

- Extrapolation on unseen, application-specific current profiles with avg. inference time of **2.55 ms** per profile $I(t)$ and diffusivity tuple (D_n, D_p) :

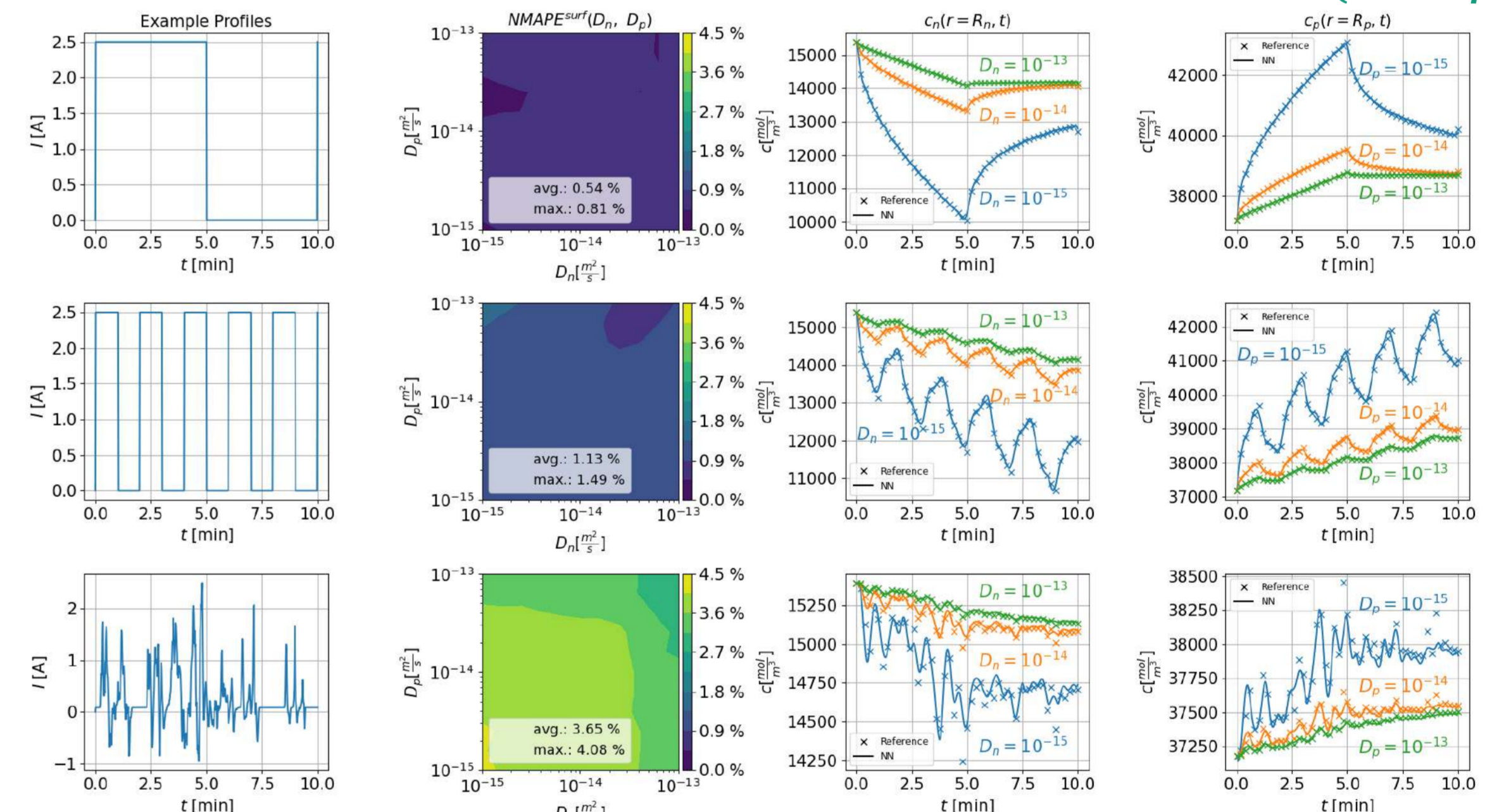


Figure 4: Extrapolation accuracy on two pulse profiles and a realistic driving profile derived from the Worldwide Harmonised Light Vehicles Test Procedure (WLTP) across diffusivity domain.

- The choice of standard deviations σ_A, σ_B determine range of frequencies in the randomized Fourier-Features, cf. Fig. 2. A related study motivated by Fourier-Transform-Analysis on the different GRF profiles is presented in Tab. 1.

$[\sigma_B^1, \sigma_B^2, \dots]$	Trunk [layers * nodes]	# total param.	NMAPE ^{surf} _{avg}
No Fourier-Features	[5*200]	1,046,802	2.42%
[10]	2 * [5*150]	1,065,302	1.37%
[100]	2 * [5*150]	1,065,302	1.17%
[1000]	2 * [5*150]	1,065,302	1.47%
[10, 100]	3 * [5*120]	1,087,682	1.12%
[10, 1000]	3 * [5*120]	1,087,682	1.15%
[10, 100, 1000]	4 * [5*100]	1,086,402	1.11%

Table 1: Study on standard deviations σ_B^i (with $\sigma_A = 1$) in temporal Fourier-Features, cf. Fig. 2. Training iterations were halved with respect to the results reported in Fig. 3 and Fig. 4 to maintain computational tractability.

Conclusion

PI-DeepONets offer potential for LIB surrogate modelling due to their fast inference times and extrapolation capabilities. Room for improvement remains in the (more) accurate approximation of high-frequency profiles and advanced architectures in branch and trunk networks for more efficient training.

See [4] for additional results on the application of PI-DeepONets for DoE.

1 Fan, G., Lu, D., Trimboli, M. S., Plett, G. L., Zhu, C., & Zhang, X. (2023). Nondestructive diagnostics and quantification of battery aging under different degradation paths. *Journal of Power Sources*, 557, 232555. <https://doi.org/10.1016/j.jpowsour.2022.232555>.

2 Andersson, M., Streb, M., Ko, J. Y., Klass, V. L., Klett, M., Ekström, H., ... & Lindbergh, G. (2022). Parametrization of physics-based battery models from input-output data: A review of methodology and current research. *Journal of Power Sources*, 521, 230859. <https://doi.org/10.1016/j.jpowsour.2021.230859>.

3 Chen, C. H., Planella, F. B., O'regan, K., Gastol, D., Widanage, W. D., & Kendrick, E. (2020). Development of experimental techniques for parameterization of multi-scale lithium-ion battery models. *Journal of The Electrochemical Society*, 167(8), 080534. <http://dx.doi.org/10.1149/1945-7111/ab9050>.

4 Brendel, P., Mele, I., Rosskopf, A., Katschnik, T., & Lorentz, V. (2025). Parametrized physics-informed deep operator networks for Design of Experiments applied to Lithium-Ion-Battery cells. *Journal of Energy Storage*, 128, 117055. <https://doi.org/10.1016/j.est.2025.117055>.

Acknowledgements:

Co-funded by the European Union under grant agreement N° 101103755 and by UKRI under grant agreement No. 10078013, respectively. Views and opinions expressed are however those of the author(s) only and do not necessarily reflect those of the European Union or the European Climate, Infrastructure and Environment Executive Agency (CINEA). Neither the European Union nor CINEA can be held responsible for them.

